Desalination and Water Treatment
www.deswater.com

doi:10.5004/dwt.2017.20972

82 (2017) 292–299
July

Performance of Li salts (LiBr + LiI + $LiNO_3$ + LiCl) for an absorption cycle of an experimental absorption heat transformer for water purification

T. Torres-Díaz[a], J. Siqueiros[b], A. Coronas[c], D. Salavera[c], A. Huicochea[a], D. Juárez-Romero[a,*]

[a]*Centro de Investigación en Ingeniería y Ciencias Aplicadas (CIICAp), Universidad Autónoma del Estado de Morelos. Av. Universidad 1001, Col. Chamilpa, Cuernavaca, Mor 62209. Mexico, Tel. +52-7773297084, e-mail: tabai.torres@uaem.mx (T. Torres-Díaz), huico_chea@uaem.mx (A. Huicochea), djuarezr7@gmail.com (D. Juárez-Romero)*
[b]*Consejo de Ciencia y Tecnología del Estado de Morelos, Subsecretaria de Innovación y Desarrollo Tecnológica La Ronda No. 13, Col. Acapantzingo, Cuernavaca. C.P. 62440 Mexico, Teléfono(s): Tel. +52 777-3121222, +52 777-3105520, e-mail: javier.siqueiros@morelos.gob.mx*
[c]*Departamento de Ingenieria Mecánica, CREVER, University Rovira i Virgili, Tarragona, Spain, e-mail: alberto.coronas@urv.cat (A. Coronos), daniel.salavera@urv.cat (D. Salavera)*

Received 30 July 2016; Accepted 24 May 2017

ABSTRACT

In this work, experimental tests were executed to analyze the performance of an absorption heat transformer using a quaternary mixture of Lithium salts (LiBr + LiI + $LiNO_3$ + LiCl) with H_2O. The high solubility of the quaternary mixture allows the operation of the absorber at a higher salt concentration than with the conventional absorption mixture water–LiBr, and the commercial absorption mixture, Carroll ™. The performance of the quaternary mixture is determined by the density and viscosity which affect the dynamic performance, while surface tension and thermal conductivity affect the heat transfer. Solubility affects the concentration range. These properties were estimated from available correlations specific for this quaternary mixture. The performance indicators studied in the absorption heat transformer were the overall specific thermal energy consumption, OSTEC, and the gross temperature lift GTL. These performance indicators were obtained for the studied quaternary mixture and compared with LiBr, and Carrol with the same absorption heat transformer. When the same absorption heat transformer (AHT) was used, the quaternary mixture produced 25% more distilled water than the LiBr. Besides, the operation of the AHT is more stable with the quaternary mixture than with LiBr or Carrol.

Keywords: Absorption fluids; Falling-film heat transfer; Absorption enhancement; Performance enhancement; Absorption heat transformer performance

1. Introduction

A practical way to purify water is evaporation. A wasted energy source can supply the required thermal energy when a heat transformer increases its temperature.

In absorption heat transformers (AHT) the LiBr-H_2O is a widely-used absorption working mixture due to its high absorption capacity as compared with others. However, because LiBr is highly active, it is also highly corrosive. Furthermore, because it has high viscosity, during the recovery of useful heat, this absorption mixture limits the overall exchange of heat and mass.

To improve the characteristics of this absorption mixture, Koo et al. [1] suggested a combination of Lithium salts and LiBr:

- $LiNO_3$ lithium nitrate, to reduce the corrosiveness; thus, it extends the useful life of the equipment.
- $LiNO_3$ and LiI, lithium iodine, to increase the solubility range; thus, the operating range of the thermal engine increases, and

*Corresponding author.

Presented at the EDS conference on Desalination for the Environment: Clean Water and Energy, Rome, Italy, 22-26 May 2016

- LiCl lithium chloride, to lower the vapor pressure of the aqueous mixture; thus, it promotes absorption.

The basic physical properties of these elements are in Appendix A. Regarding the proportion of each salt Koo et al. [1] used the solubility as criteria: thus, these authors found adequate a molar ratio of [LiBr:$LiNO_3$, LiI] of (5:1:1). The ratio of LiCl was selected to lower the vapor pressure. Also, Koo et al. [2] experimentally determined densities, viscosities and surface tension of this mixture in the ranges 10 < T< 60°C and 50< x <65. %wt. Later on Lee et al. [3] constructed the Dühring and the enthalpy-concentration diagrams for this working mixture. Epelde et al. [4] evaluated the thermo-physical properties of this quaternary mixture in the ranges 0 < T < 120°C and 40 < x < 70 %wt. Moreover, recently Asfand and Bouronis [5] estimated the heat of dilution for this quaternary mixture.

Thus, the aim of this work is:

- To compare the performance of the quaternary mixture with the performance of LiBr-H_2O as studied by Huicochea et al., 2009 [6] and Carrol mixtures, as studied by Torres-Diaz, 2013 [7] in the same AHT
- To compare the operation of the quaternary mixture with the operation of LiBr and Carrol mixtures in the same AHT.

Table 1 compares previous works related to absorption pumps operating with this quaternary mixture composed by Lithium Bromide +Lithium Iodide + Lithium Nitrate + Lithium Chloride (mol ratio 5:1:1:2).

Advances in water purification by AHT are presented in table 2.

Derived from the theoretical work of Bourouis et al. [10] the absorption mixture selected is an aqueous solution of LiBr+LiI+$LiNO_3$+LiCl.

Bourouis et al. [8] observed that when the salt concentration increases from 61.0 to 64.2%, the absorption thermal load increases about 28% with respect to LiBr at 57.9%wt. However, the heat and mass transfer coefficients hardly change. Thus, a salt concentration of 64.2 %wt.is recommended for the AHT.

2. Experimental layout

An absorption heat transformer for water purification consists of a generator, an absorber, an economizer, an

Table 1
Comparison of the performance of absorption working mixtures in heat pumps

Authors	Equipment	Absorption mixture	Operating conditions	Findings
Bourouis et al. 2005 [8]	Vertical falling tube absorber at air-cooling thermal conditions	LiBr 57.9%wt for LiBr. 61.0, and 64.2 wt% for the quaternary mixture	P = 1.3 kPa T_c = 35°C. common 75 ≤ Re ≤ 175. (wavy-laminar) Due to the higher viscosity of the quaternary mixture	0.2 ≤ α ≤ 0.6kW/m² K for the LiBr and the quaternary salt mixture. $2.6 \times 10^{-5} \leq \beta \leq 9.0 \times 10^{-5}$ m/s for LiBr $2.0 \times 10^{-5} \leq \beta \leq 4.40 \times 10^{-5}$ m/s (61.0 %wt) $2.7 \times 10^{-5} \leq \beta \leq 3.7 \times 10^{-5}$ m/s (64.2 %wt) for quaternary salt mixture.
Yoon et. Al. 2005 [9].	A helical absorber	LiBr-H_2O n-Octanol (40–50% wt), and the quaternary salt mixture (45–59 %wt).	10.73 kPa 0.01 ≤ Γ ≤ 0.04 Kg/m s. Cooling: W_c = 0.216 kg/s, T_c = 30.35°C	Heat flux increases 5–7% in the quaternary salt compared to LiBr. Recommended Γ of the quaternary salt is 0.03 kg/s m

Table 2
Advances in water purification by absorption heat transformers

Reference	Equipment	Absorption mixture	Operating conditions	Findings
Bourouis et al. 2004 [10].	Simulation	LiBr-H_2O	$10 \leq T_{CO} \leq 40$ $60 \leq T_{EV} \leq 80$	Better COP is expected with the quaternary salt compared to LiBr-H_2O. The wider range of solubility of quaternary salt makes possible the operation of the AHT at higher concentrations.
Sekar and Saravanan, 2011 [11].	LiBr. horizontal generator, a vertical absorber	LiBr-H_2O	$24 \leq P_{CO} \leq 3.1$ $20 \leq T_{CO} \leq 25$ $12 \leq P_{Ev} \leq 12.8$ $60 \leq T_{EV} \leq 80$	$1.6 \leq W_{Wp} \leq 4$kg/h

evaporator and a condenser. These main components are made of 316 L stainless steel. This AHT as shown in Fig. 1. has a design capacity of 700 W, with an overall size of 0.80 × 1.20 × 1.60 m. The water purification circuit is made of copper and stainless steel. The generator and the absorber are shell-and-tubes heat exchangers. The generator and the absorber operate as a falling film exchangers with horizontal tubes. The economizer is a double concentric, coil-shaped tube heat exchanger with 4 turns. The condenser and the evaporator are also double concentric coil-shaped tubes heat exchangers. A thermal insulator made of an expanded elastomer with a thermal conductivity of 0.040 W/m K was used.

The heat supplied by the generator and the evaporator is provided by a thermal bath with a regulated heating coil. The released heat in the absorber was gained by the water purification cycle, which uses a magnetic pump with variable speed from 0 to 5600 rpm. The absorption mixture circulates with a centrifuge pump at 3450 rpm. The heat was extracted from the condenser with an external circuit by using a centrifuge pump also at 3450 rpm.

Fig. 1. Experimental absorption heat transformer coupled for water purification.

The cycle operates at two pressure levels: high and low. Fig. 2 shows a schematic diagram of an absorption heat transformer represented in a pressure-temperature chart. A warm waste stream supplies an amount of heat $\dot{Q}_{GE}$ at temperature T_{GE} to the generator to evaporate part of the refrigerant from the weak solution. This evaporated refrigerant flows to the condenser delivering an amount of heat $\dot{Q}_{CO}$ at the low temperature T_{CO}. The liquid refrigerant which leaves the condenser is pumped to the evaporator in the high-pressure zone. The refrigerant is then evaporated by using a quantity of waste heat $\dot{Q}_{EV}$ that is added to the evaporator at a temperature T_{EV}. Next, the evaporated refrigerant flows to the absorber where it is absorbed by the strong solution of absorbent which comes from the generator. This reaction delivers a heat $\dot{Q}_{AB}$ at a high temperature T_{AB}. Finally, the weak solution returns to the generator after preheating the rich solution in the economizer and it repeats the cycle.

There are several characteristics to be considered in the operation of an AHT for water purification:

- The mass flow rate per unit length of the solution in the absorber and in the generator is regulated to produce an adequate wetting; thus, heat release is enhanced.
- Recirculation also recovers some absorption heat released by absorption in the re-collector.
- The water stream to be purified circulates inside the pipes of the absorber and it evaporates there. The production of distilled water is very sensitive to the configuration of streams (due to the thermal gradients) and to the thermodynamic properties of the film operating conditions. During the operation, the product can be trapped in the liquid phase due to sudden pressure changes profiles, or temperature profiles along the equipment; thus, the production of the distillate could decrease.

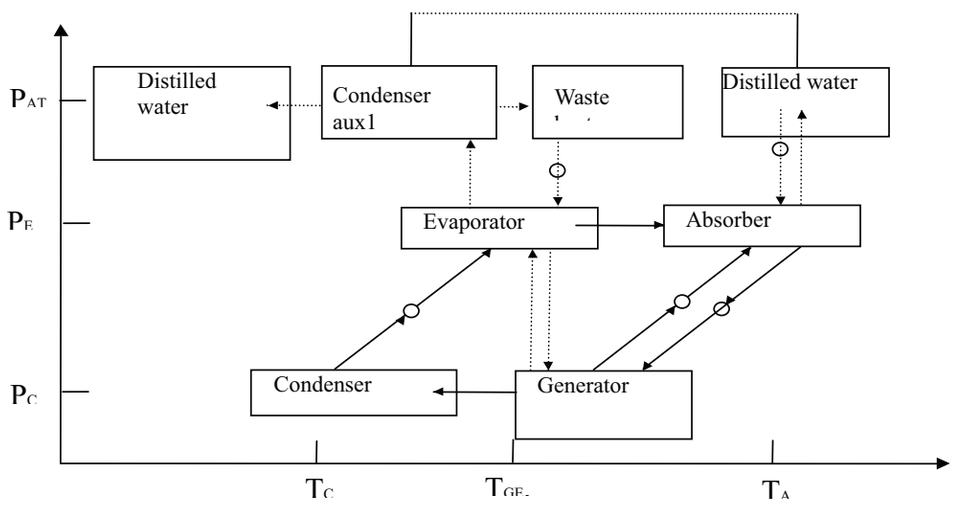

Fig. 2. Diagram of an absorption heat transformer.

The design characteristics of the generator and the absorber appear in Table 3.

The absorber has four passes, in a concentric configuration. The hottest point is near the outlet of the distilled stream to enhance the production of purified water.

3. Energy and mass balances in the AHT

3.1. Balance equations

Heat supplied in the generator for hot stream

$$\dot{Q}_{GE} = W_{GE} Cp_{GE} (T_{GE,In} - T_{GE,Out})$$

Heat dissipated in the condenser for cold stream

$$\dot{Q}_{CO} = W_{CO} Cp_{CO} \left(T_{CO,Out} - T_{CO,In}\right)$$

Heat supplied to the evaporator for hot stream

$$\dot{Q}_{EV} = W_{EV} Cp_{EV} \left(T_{EV,In} - T_{EV,Out}\right)$$

Table 3
Design characteristics of the generator and the absorber for water purification

GENERATOR Stainless Steel 316 L	
Design capacity	1.9 kW
Configuration	Cross current. Two-pass.
Distributor	5 pipes, horizontal.
Diameter	0.00635 m
Hole size	0.0095 m
Spacing between pipes	0.009 m
Shell diameter	0.1524 m
Diameter of shell, flanged	1.02 m
Pipe length	0.600 m
Pipes per row from top	5, 6,7, 6, 5, 4
Pipe diameter	0.0095 mm
Heat Transfer area	0.59 m

ABSORBER. Stainless Steel 316 L	
Design capacity	0.8 kW
Configuration	Crosscurrent. Four-pass.
Distributor	5 horizontal pipes
Distributor diameter	0.00635 m
Hole size	0.0024 m
Spacing	0.009 m
Shell size	1.02 m internal
Pipes length	0.400 m
Pipes per row: (from top)	4, 5, 4, 3
Pipe diameter	0.0095 m
Pitch	Triangular 0.005 m
Heat Transfer area	0.2 m

Useful heat applied to the saline stream

$$\dot{Q}_{AB} = W_{AB} Cp_{AB} (T_{AB,In} - T_{AB,Sat}) + W_{AB,Rfr} \Delta H_{Vap}$$

3.2. Transient performance

The film thickness, δ, of the absorption mixture is given by:

$$\delta = \left(\frac{3\mu_f \Gamma}{\rho_l^2 g \sin(\theta)}\right)^{1/3} = \left(\frac{3\mu_f{}^2 \mathrm{Re}_f}{4\rho_l^2 g \sin(\theta)}\right)^{1/3}$$

where θ is the angle of the flow with respect to the vertical.

For a flow per unit length, Γ, the film Reynolds is evaluated as:

$$\mathrm{Re}_f = \frac{4\Gamma}{\mu_f}$$

Then, the film temperature changes as:

$$M_f Cp_f \frac{dT_f}{dt} = Q_{Hot} - Q_{Trn}$$

$$M_f = \delta\ A_{Trn} \rho_f$$

3.3. Criteria of performance

We considered three performance indices:

The ratio of heat obtained and heat supplied, COP.

$$COP = \frac{\dot{Q}_{AB}}{\dot{Q}_{GE} + \dot{Q}_{EV}}$$

The gross temperature lift between absorber and evaporator.

$$GTL\ = T_{AB,Sln} - T_{EV,Rfr}$$

The heat energy consumed by the AHT per unit of purified water product.

$$OSTEC = \frac{\dot{Q}_{GE} + \dot{Q}_{EV}}{W_{AB,Dsw}}$$

As introduced by Sekar and Saravanan, (2011), [11].

3. Results and discussion

Here we present the decommissioning results of the quaternary mixture compared to Lithium Bromide and to Carrol. Table 4 shows a comparison of operating conditions for these three absorption mixtures. The pressure of the absorber with the quaternary mixture is the lowest compared to LiBr and to Carrol.

The COP with the quaternary mixture is lower than with LiBr, and Carrol. However, the production of purified water is 25% higher with the quaternary mixture than with LIBr; but it is lower than with Carrol.

Fig. 3 shows the experimental outlet temperatures of the main component of the AHT with the quaternary solution. With this absorption mixture,the AHT smoothly arrives to steady state conditions. The time for a steady state of temperature for this mixture was 3 h. LiBr and Carroll arrive to steady state after 2 h.

Table 4
Comparison of operating conditions of the main components with LiBr, Carrol and the quaternary mixture

	LiBr Huicochea [6]	Carrol Torres-Diaz [7]	Quaternary mixture. This work (2016)
T_{GE}, °C	81.5–92.2	86.7–89.5	87.2–89.9
T_{CO}, °C	23.1–28.5	23.5–27.8	21.9–22.9
T_{EV}, °C	77.3–84.3	70.2–74.7	77.5–81.7
T_{AB}, °C	96.0–100.8	96.8–101.0	97.5–98.6
P_{GE}, kPa	8.1–9.6	8.4–9.1	6.7–7.1
P_{AB}, kPa	26.2–31.8	36.4–55.9	28.6–30.8
COP (–)	0.150–0.231	0.247–0.334	0.120–0.167
$\dot{Q}_{AB}$ (kW)	0.233–306	0.262–0.598	0.387–0.440
Maximum distilled water mL/h	277	788	348

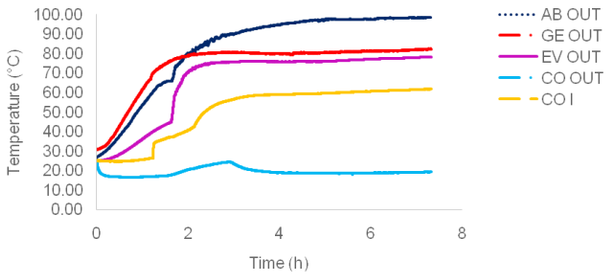

Fig. 3. Behavior of experimental outlet temperatures of the four components of the AHT with the quaternary mixture.

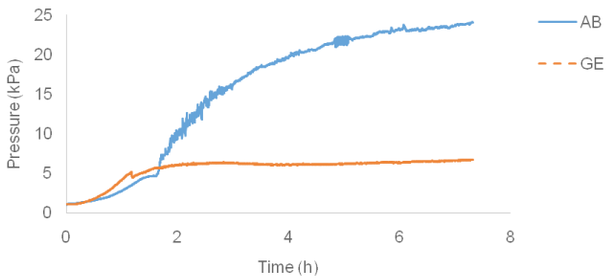

Fig. 4. Pressure in the generator and the absorber of the AHT.

Fig. 4 presents the pressure in the Generator and in the Absorber of the AHT.

The generator and the absorber start at sub-atmospheric pressure. After 90 min the absorption mixture is heated in the generator; thus, it increases its vapor pressure. As the concentrated mixture travels through the economizer, it arrives at the absorber where the drops of concentrated mixture contact the evaporated refrigerant. Then, the absorption mixture releases heat, and increases its vapor pressure. A fraction of this heat is used to evaporate the saline water, and the other fraction is used to heat the absorption mixture. As a result, the absorber increases its pressure at a level higher than that of the generator. After 420 min the pressure in the generator is stable, while the pressure in the absorber tends asymptotically towards stability.

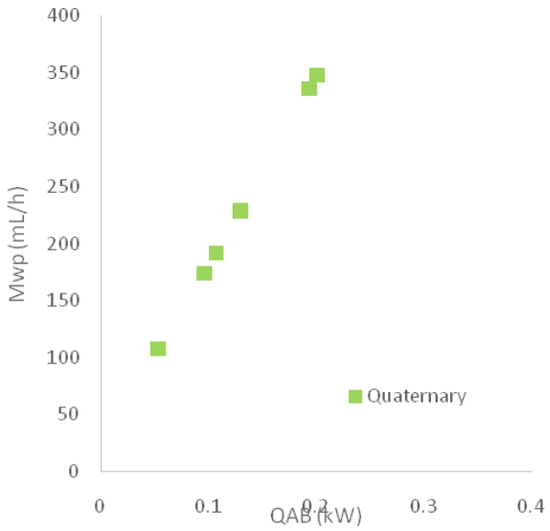

Fig. 5. Distillate behavior vs. heat supplied in the absorber.

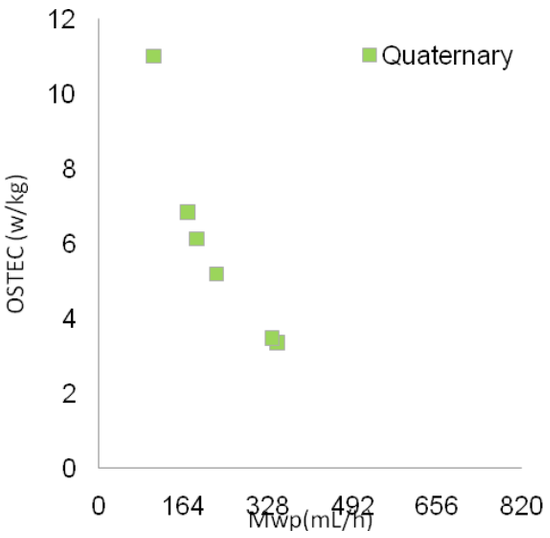

Fig. 6. OSTEC behavior vs. water purification with the quaternary mixture.

Fig. 5 shows a linear behavior of the distillate against the heat produced in the absorber for the quaternary absorption mixture.

Fig. 6 shows the OSTEC vs. distilled water for the quaternary absorption mixture. The OSTEC, requirements decrease as distillate production increases. The quaternary salt has slightly smaller OSTEC than LiBr. If film thickness increases, it is expected that heat transfer decreases, but the dynamic is steadier (see equations for transient performance), compared to LiBr. Film thickness of the quaternary salt is greater than LiBr-H_2O, since the film acts as a thermal inertia for the heat transfer process.

Fig. 7 shows the behavior COP vs. the temperature difference between the absorber and the evaporator, GTL. The absorption mixture favors a lower temperature difference between the absorber and the evaporator to improve the COP. The highest COP = 0.167 at GTL = 15.84°C.

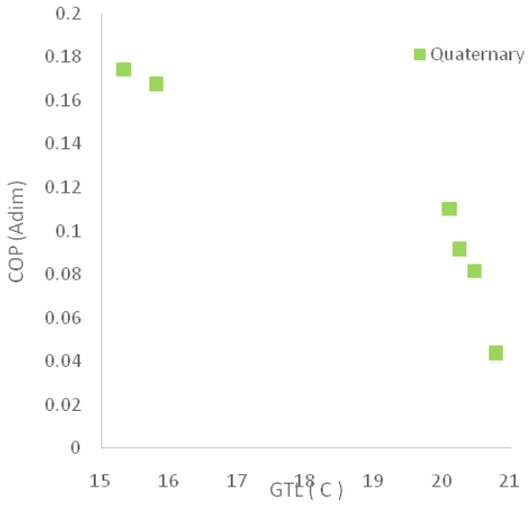

Fig. 7. Temperature of the GTL vs. COP

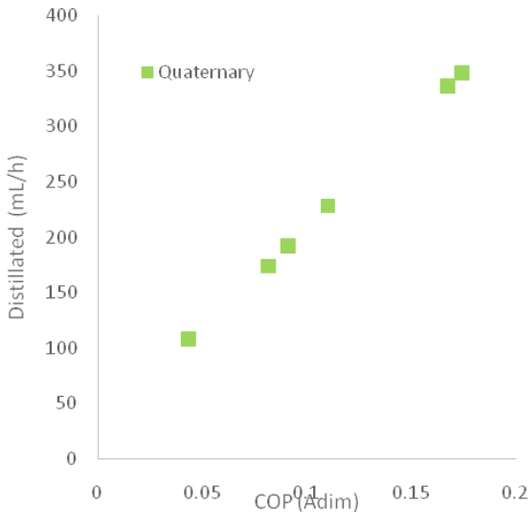

Fig. 8. Behavior of distilled water vs. COP with the quaternary mixture.

Fig. 8 shows the behavior of Distilled vs. COP. The quaternary mixture presents amonotonic increase of distilled water as COP increases. Table 5 presents the physical and transport properties at their best-operating conditions. The physical properties of the LIBr, Carrol, and the quaternary mixture were obtained from correlations developed by Torres-Merino, 1997 [12], Carrol Co.1984, [13], and Salavera, 2004 [14].

The AHT produced 25.6 % more distilled with quaternary mixture than with LiBr. This is a consistent result, comparable to the 28% improvement obtained in an air cooled absorption chiller by Bourouis et al. [8]

In our experimental lay-out the flow of the quaternary mixture from the absorber to the generator limits the performance. This flow is limited because:

- The pressure drop between absorber and generator is low.
- At the operating conditions, the quaternary mixture has higher viscosity and density than the other two absorption mixtures. The effect of these properties is more sensitive along the pipe of the economizer.

The mass flow rate of AB-GE presents fluctuations with LiBr and Carrol due to is enthalpic expansion. This flow has a strong interaction between supplied heat and pressure differences (due to the vapor pressure) and holdup. The quaternary salt is less sensitive to this pressure differences than LiBr or Carrol (since LiCl acts as a vapor pressure suppressor) and holdup variations (since this mixture has the highest density). Therefore, this mixture does not present considerable flashing during the operation.

Carrol and LiBr aqueous mixtures are highly dependent on the suction pressure during startup, while the quaternary mixture is less sensitive to this pressure.

4. Conclusions

4.1. Performance

The quaternary mixture purifies more than 25% of distilled water compared to LiBr. Carrol produced the greatest amount of distilled water. Preliminary experimental results showed that the OSTEC performance of the quaternary solution is between Carrol and LiBr. Carrol also produces the highest-pressure difference between the generator and the absorber.

4.2. Operation

Startup is slower with the quaternary salt than with LiBr or Carrol, but it is more stable. It presents low sensi-

Table 5
Comparison of physical and transport properties of absorption mixtures at their best production of distilled water, with the same AHT

	Temp °C	Conc. %	Viscosity Pa·s	Density kg/m^3	ΔP AB-GE kPa	Vapor pressure kPa	Distilled water ml/h
LiBr	98.40	54.20	0.00140	1561.90	23.78	21.48	277
Carrol	100.45	58.25	0.00190	1471.83	43.75	29.52	788
Quaternary	98.27	61.78	0.00218	1644.35	24.13	12.37	348

tivity to changes in the operation pressures and to fluctuations of the holdup in the absorber. Thus, the quaternary salt is more suitable for attenuation of disturbances during the operation.

Acknowledgements

T. Torres-Diaz is indebted with CREVER for his student visit, and to CONACyT for his mobility grant.

Symbols

A	—	Area, m^2
C_p	—	Heat capacity, kJ/kg°C
g	—	Gravity acceleration, m/s^2
P	—	Pressure, kPa
Q	—	Heat flow rate, kW
T	—	Temperature °C
W	—	Mass flow rate, kg/s

Greek

α	—	Heat transfer coefficient, kW/m^2 K
β	—	Mass Transfer coefficient
δ	—	Film thickness, m
Γ	—	Flow per unit length, Kg/s m
μ	—	Dynamic viscosity, kg/m s
θ	—	Angle with respect to vertical, radians
ρ	—	Density, kg/m^3

Subscripts

AB	—	Absorber
c	—	Cooling
Cld	—	Cold stream
f	—	Film
CO	—	Condenser
Dsw	—	Distillated water
EV	—	Evaporator
GE	—	Generator
Hot	—	Hot stream
IN	—	Input
OUT	—	Output
Rfr	—	Refrigerant
Trn	—	Transfer

References

[1] K.K. Koo, H.R. Lee, S. Jeong, Y.S. Oh, D.R. Park, Y.S. Baek, Solubilities, vapor pressures and heat capacities of the water + lithium bromide + lithium nitrate + lithium iodide + lithium chloride system, Intl. J. Thermophysics, 20(2) (1999) 589–600.

[2] K.K. Koo, H.R. Lee, Y.S. Oh, D.R. Park, Y.S. Baek, Densities, Viscosities, and surface tensions of the (water + lithium bromide + lithium nitrate + lithium iodide + lithium chloride) system, J. Chem. Eng. Data, 44 (1999) 1176–1177.

[3] H.-R. Lee, K.-K. Koo, S. Jeong, Y.-S. Oh, D.-R. Park, Y.-S. Baek, Thermodynamic design data and performance evaluation ofthe water + lithium Bromide + lithium Iodide + lithium nitrate + lithium chloride system for absorption chiller. Appl. Therm. Eng., 20 (2000) 707–720

[4] M. Epelde, S. Steiu, J. Mesones, D. Salavera, A. Coronas, Thermophysical properties of H_2O + (LIBr + $LiNO_3$ + LiI + LiCl) mixture for absorption refrigeration, 4th IRR Conf. Thermophysical Properties and Transfer Process Refrigerants, Delf, NL. Paper TP-082 (2013).

[5] F. Asfand, M. Bourouis, Estimation of differential heat of dilution for aqueous lithium (bromide, iodide, nitrate, chloride) solution and aqueous (lithium, potassium, sodium) nitrate solution used in absorption cooling system, Intl. Refrig., 75 (2016) 18–25.

[6] A. Huicochea, J. Siqueiros, Increase of COP for an experimental heat transformer using a water purification system, Desal. Water Treat., 12 (2009) 305–312.

[7] T. Torres-Diaz, Experimental study on an absorption heat transformer, and an evaporation process with heat recycling, Thesis UAEM (Spanish). (2013).

[8] M. Bourouis, M. Vallès, A. Medrano, Coronas absorption of water vapor in the falling film of water–(LiBr + LiI + $LiNO_3$ + LiCl) in a vertical tube at air-cooling thermal conditions, Int. J. Thermal Sci., 44 (2005) 491–498.

[9] J. Yoon, O. Kwon, C. Moon, H. Lee, P. Bansal, Heat and mass transfer characteristics of a helical absorber using LiBr and LiBr + LiI + $LiNO_3$ + LiCl solutions, Intl. J. Heat Mass Trans., 48 (2005) 2102–2109.

[10] M. Bourouis, A. Coronas, R.J. Romero, J. Siqueiros, Purification of seawater using absorption heat transformer with water-(LiBr + LiI + $LiNO_3$ + LiCl) and low temperature heat sources, Desalination, 166 (2004) 209–214.

[11] S. Sekar, R. Saravanan, Expérimental studies on absorption heat transformer coupled distillation system, Desalination, 274(1) (2011) 292–301.

[12] J. Torres-Merino, Contacteurs Gaz-Liquide pour Pompes a Chaleur á Absorption Multi- Étagés, Ph.D. Thesis, France. L'Inst. Nat.l Polytechnique de Lorraine, France, 1997.

[13] Carrier Corp. Development of a Single-Family Absorption Chiller for use in a Solar heating and Cooling system. Phase3, Final Report v 1. Syracuse, Ny. Energy Sys. Div.1984.

[14] D. Salavera, X. Esteve, K.R. Patil, A.M. Mainar, A. Coronas, Solubility, heat capacity, and density of lithium bromide +lithium Iodide + lithium nitrate + lithium chloride aqueous, solutions at several compositions and temperatures, J. Chem. Eng. Data, 49 (2004) 613–619.

Appendix A

Physical properties of the elements composing the quaternary mixture

Table A.1
Physical properties of the elements composing the quaternary mixture

Salt	Molecular weight g/mol	Mol ratio	Density g/cm^3	Boiling Point °C
LiBr	88.845	5	3.460	1265
LiI	133.845	1	4.076	1171
$LiNO_3$	68.945	1	2.380	873
LiCl	42.394	2	2.070	1382